



**A computational study of regioselectivity in aluminum hydride ring-opening of *cis*- and *trans*- 4-*t*-butyl and 3-methylcyclohexene oxides**

Journal:	<i>Organic &amp; Biomolecular Chemistry</i>
Manuscript ID	OB-ART-07-2019-001675.R1
Article Type:	Paper
Date Submitted by the Author:	05-Sep-2019
Complete List of Authors:	Deora, Nipa; Borough of Manhattan Community College, Science Carlier, Paul; Virginia Polytechnic Institute and State University, Chemistry

## ARTICLE

## A computational study of regioselectivity in aluminum hydride ring-opening of *cis*- and *trans*- 4-*t*-butyl and 3-methylcyclohexene oxides

Received 00th January 20xx,  
Accepted 00th January 20xx

DOI: 10.1039/x0xx00000x

Nipa Deora,<sup>\*a</sup> and Paul R. Carlier<sup>b</sup>

Nucleophilic ring opening of cyclohexene oxides is known to proceed preferentially through the *trans*-diaxial pathway (the Fürst-Plattner rule). This preference, however, is not absolute, and can be affected by substituents on the cyclohexene oxide ring, as illustrated by LiAlH<sub>4</sub> ring-opening of the *cis*- and *trans*-isomers of 4-*t*-butyl- and 3-methylcyclohexene oxide (*cis*- and *trans*-1, *cis*- and *trans*-2). We performed B3LYP/6-31+G\*(PCM) geometry optimizations to locate the chair-like and twist-boat-like transition structures for the hydride attacks on the pseudoaxial and pseudoequatorial conformers of these epoxides. Our calculations are consistent with the experimental observation of effective Fürst-Plattner control of AlH<sub>4</sub><sup>-</sup>-opening of *cis*-1, *trans*-1, and *cis*-2, but low selectivity in ring-opening of *trans*-2. Our data at B3LYP/6-31+G\*(PCM) suggests this reduction in selectivity is due to a diminished pseudoequatorial preference of the 3-methyl group in *trans*-2 relative to that in *cis*-2. The two calculated chair-like transition structures for hydride opening of *trans*-2 differ in activation energy free energy ( $\Delta\Delta G^\ddagger$ ) by only 0.4 kcal/mol. Thus, these calculations account for the reduced regioselectivity of ring opening seen for *trans*-2 by AlH<sub>4</sub><sup>-</sup> and other nucleophiles.

### Introduction

Cyclohexene oxides feature prominently in natural product and steroid chemistry.<sup>1-3</sup> Nucleophilic ring opening of cyclohexene oxides normally proceeds with high regioselectivity as governed by the Fürst-Plattner or “*trans*-diaxial” effect.<sup>4</sup> As shown computationally by Nakamura and Morokuma,<sup>5</sup> Fürst-Plattner control of ring opening can be attributed to a preference for a chair-like transition state (giving the *trans*-diaxial product) rather than a twist-boat-like transition state (which would give the diequatorial product). Whereas cyclohexene oxide equally populates two enantiomeric half-chair conformers, monosubstituted cyclohexene oxides will favor the half-chair that places the substituent in a pseudoequatorial position. Thus a number of studies have shown that the magnitude of Fürst-Plattner control can be modulated by the position, size and orientation of alkyl substituents.<sup>6-10</sup> In addition, in Lewis Acid-mediated ring opening of cyclohexene oxides, regioselectivity can be affected by chelating groups.<sup>11-16</sup>

Most relevant to our study, Rickborn and coworkers reported the regioselectivity of LiAlH<sub>4</sub> ring-openings of *cis*- and *trans*- 4-*t*-butylcyclohexene oxide (*cis*-1 and *trans*-1) and *cis*-

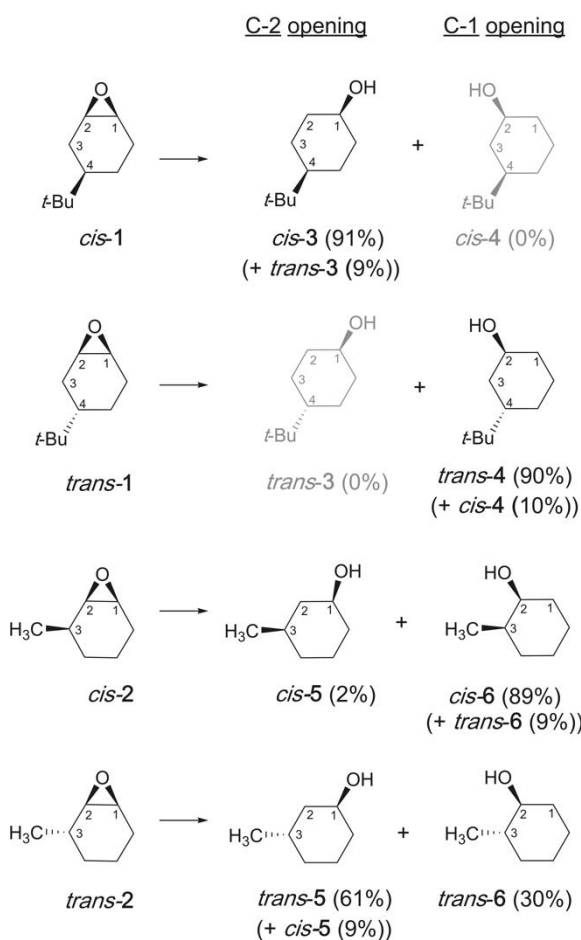
and *trans*-3-methylcyclohexene oxide (*cis*-2 and *trans*-2).<sup>6, 10</sup> Scheme 1 represents the extrapolated data from both these studies. In some cases, pure diastereomeric epoxides could not be isolated and thus reactions of a range of diastereomeric mixtures were used to extrapolate the product ratio that would have been obtained from the diastereomerically pure epoxide. These extrapolated regioselectivities are depicted in Scheme 1, and in 3 of 4 cases indicate near-exclusive formation of the product of *trans*-diaxial addition of hydride to alkyl-pseudoequatorial conformer of the corresponding epoxide. Thus, hydride opening of *cis*-1 gave 100% C2-opening, consistent with Fürst-Plattner control: *cis*-3 was obtained in 91% yield, and its epimer *trans*-3 was isolated in 9% yield. Subsequent experiments with LiAlD<sub>4</sub> gave d<sub>2</sub>-*trans*-3, suggesting that *trans*-3 resulted from C1-hydride transfer from *cis*-3-Li (the lithium alkoxide of *cis*-3) to AlH<sub>3</sub> in situ (forming 4-*t*-butylcyclohexanone and regenerating AlH<sub>4</sub><sup>-</sup>) followed by reduction of the ketone.<sup>10</sup> In any event, no products of C-1 opening were seen. Similarly, *trans*-1 reacted with LiAlH<sub>4</sub> in 100% Fürst-Plattner control, giving C-1 opening products *trans*-4 in 90% yield, and the epimer *cis*-4 in 10% yield (presumably originating by the same mechanism that gave *trans*-3 from *cis*-1). Once again, none of the C-2 opening product *trans*-3 was isolated.<sup>10</sup>

<sup>a</sup> Department of Science, CUNY, Borough of Manhattan Community College, New York, NY 10007. Email: [ndeora@bmcc.cuny.edu](mailto:ndeora@bmcc.cuny.edu)

<sup>b</sup> Department of Chemistry, Virginia Tech, Blacksburg, VA 24061

Electronic Supplementary Information (ESI) available: Cartesian coordinates for select optimized structures (B3LYP/6-31+G\*(PCM), single point energies, electronic energies, ZPVE and G<sub>corr</sub> for all calculated species. See DOI: 10.1039/x0xx00000x

**Scheme 1:** Regioselectivity of reactions of (*cis*- and *trans*- **1** and **2**) with LiAlH<sub>4</sub>. In the case of *cis*-**1** and *trans*-**2**, the depicted regioselectivity was extrapolated from experiments on *cis*-/*trans*- mixtures.<sup>6,7</sup>

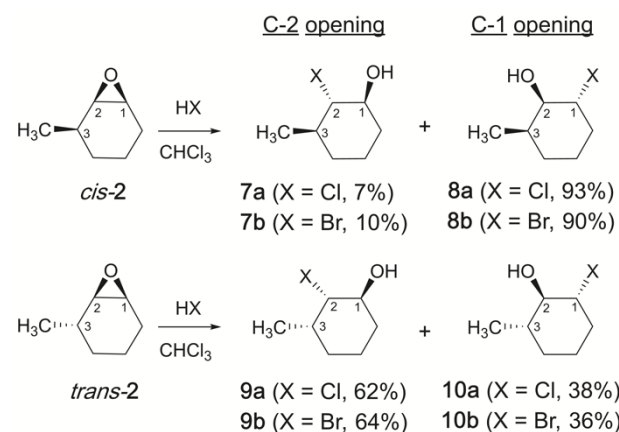


All reactions carried out with i) LiAlH<sub>4</sub>, Et<sub>2</sub>O ii) HCl(aq).

For the *cis*-3-methyl system *cis*-**2**, products *cis*-**5** and *cis*-**6** were formed in 2:89 ratio, and the epimer *trans*-**6** was also obtained. Thus for *cis*-**2**, the Fürst-Plattner:anti-Fürst-Plattner ratio is again very high, 98:2. Interestingly however, for *trans*-**2**, the reaction was much less selective, and a 61:30 ratio of the ring opening products *trans*-**5** and *trans*-**6** was obtained, along with 9% of epimer *cis*-**5**. The moderate preference for C2-opening (70:30) can once again be explained on the basis of preferred axial attack on the C2 carbon of the methyl-pseudoequatorial conformer of *trans*-**2**. Rickborn and co-workers proposed that the unexpectedly significant regioisomer *trans*-**6** most likely formed by *trans*-diaxial addition of hydride to C1 of the methyl-pseudoaxial conformer of *trans*-**2**. Intervention of the twist-boat-like transition structure was considered less probable by the authors.

A similar dichotomy in ring-opening selectivity for *cis*-**2** and *trans*-**2** was also seen by Bellucci and coworkers, who studied the ring openings with HCl and HBr in chloroform (Scheme 2).<sup>8, 9</sup> As was seen for hydride-opening, regioselectivity for *cis*-**2** was high. Addition of HCl gave **8a** and **7a** in a 93:7 ratio, and addition of HBr gave **8b** and **7b** in a 90:10 ratio. Thus in both cases, the major product results from *trans*-diaxial addition of halide to the methyl-pseudoequatorial

**Scheme 2:** Ring opening regioselectivity of *cis*- and *trans*-**2** with HCl and HBr.<sup>8,9</sup>



conformer of *cis*-**2**•H<sup>+</sup> (likely protonated). However, significantly lower regioselectivities were once again observed in reactions of *trans*-**2**. Addition of HCl gave **9a** and **10a** in a 62:38 ratio, and addition of HBr gave **9b** and **10b** in a 64:36 ratio. Bellucci et al. explained this lack of selectivity for *trans*-**2** differently than Rickborn et al., suggesting that approach of the attacking nucleophile to C2 of *trans*-**2** occurred in an 'oblique' fashion instead of perpendicular one, a path that would be adversely affected by a *trans*-3-substituent.

To date, a limited number of computational studies have addressed selectivity in ring-opening of cyclohexene oxides.<sup>5, 12, 16-18</sup> The first of these was by Nakamura and Morokuma who investigated the ring opening of cyclohexene oxides with MeCuLi•LiCl.<sup>5</sup> In their pioneering work, they located the ring opening chair-like and twist-boat-like transition structures, and provided a theoretical explanation for the *trans*-diaxial preference. Angalada and Delgado analyzed the effects of chelation by LiClO<sub>4</sub> to predict the ring opening energetics of benzyloxy substituted cyclohexene oxides in their work on regioselective synthesis of aminocyclitols.<sup>12</sup> Calculations on the ring openings of 1-methylcyclohexene oxide and limonene oxide were performed by Himo and coworkers in their study on the catalytic mechanism of limonene epoxide hydrolase.<sup>17</sup> Fürst-Plattner ring opening pathways were explored by Houk and Jung to explain the selectivities observed for non-aldol aldol rearrangements of isomeric 6-methyl-2,3-epoxycyclohexyl silyl ethers with TESOTf.<sup>18</sup> Computational studies were also performed by Taylor and coworkers during their work on boronic acid catalyzed ring opening of *cis*-3-hydroxycyclohexene oxides with acyl chloride.<sup>16</sup> Yet despite the extensive use of LiAlH<sub>4</sub> in synthesis to reduce epoxides, to the best of our knowledge, there are no computational studies that have addressed the regioselectivity of LiAlH<sub>4</sub> ring-opening of cyclohexene oxides. In this paper, we analyze the ring opening of 4-*t*-butyl and 3-methyl substituted cyclohexene oxides (*cis*- and *trans*-**1**, and *cis*- and *trans*-**2**) with LiAlH<sub>4</sub> using density functional and MP2 methods. The results obtained account for the high regioselectivities seen for *cis*-**1**, *trans*-**1**, and *cis*-**2**, and provide an explanation for the low selectivity seen with *trans*-**2**.

## Computational Methods

All calculations were performed using Gaussian 09:<sup>19</sup> the B3LYP functional<sup>20</sup> and 6-31+G\* basis set were used to calculate geometries and frequencies. All calculations were performed using the default grid option (Integral=FineGrid) for B3LYP in Gaussian 09. Fine grid is a pruned (75,302) grid with 75 radial shells and 302 angular points per shell. All stationary points were characterized by vibrational frequency analysis as minima (zero imaginary frequencies) or as transition structures (with one imaginary frequency). Animation of the sole imaginary frequencies of located transition states confirmed their location on the reaction coordinate between the epoxide-Li<sup>+</sup> complexes and the ring-opened products. Since available experimental data are solution-based, effects of bulk solvation were incorporated by using the Polarized Continuum Model (PCM) with ether as the solvent during geometry optimizations, which we denote as B3LYP/6-31+G\*(PCM).<sup>21-23</sup> Activation free energies obtained were used to calculate the  $k_i/k_s$  ratios for attacks at C1 and C2 carbons. These ratios were then applied to predict the ratio of products obtained.<sup>24</sup> Single point calculations were performed using the larger basis set at B3LYP/6-311+G(2d,p)(PCM), mPW1PW91/6-311+G(2d,p)(PCM) and using wb97xd/6-31+G\*(PCM) method and basis on the B3LYP/6-31+G(d)(PCM) optimized geometries. Our previous work on epoxides has shown that in some cases, B3LYP may not provide accurate results, and should ideally be benchmarked against post-Hartree-Fock methods, so single point calculations were performed at MP2/6-31+G\*(PCM).<sup>25</sup> Free energy corrections were obtained from frequency calculations on the B3LYP/6-31+G\*(PCM) geometries and applied to calculate the free energies for the single point calculations performed in this study. Molecular graphics were created using USCF Chimera visualization system.<sup>26</sup>

## Results and Discussion

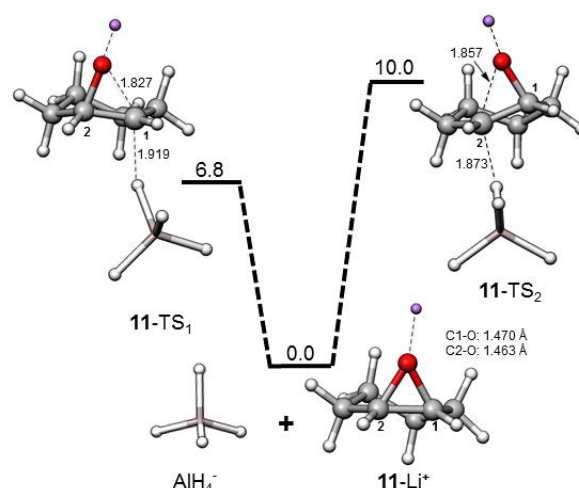
Before starting our ring opening investigations on substituted cyclohexene oxides, we investigated reaction of unsubstituted cyclohexene oxide, **11** with LiAlH<sub>4</sub>. To assess the importance of Li<sup>+</sup> assistance in ring-opening, we located transition structures for ring opening of both **11** and **11-Li<sup>+</sup>** by AlH<sub>4</sub><sup>-</sup>, at B3LYP/6-31+G\*, using a continuum solvation model (PCM, Et<sub>2</sub>O). As expected, ring-opening of the neutral **11** gave large activation free energies ( $\Delta G^\ddagger$ ) values of 30.2 (chair-like transition state) to 34.2 kcal/mol (twist-boat-like transition state), Table 1).

**Table 1:** Free energies of activation ( $\Delta G^\ddagger$ ) at B3LYP/6-31+G\*(PCM) in ether for ring opening of **11** and **11-Li<sup>+</sup>** with AlH<sub>4</sub><sup>-</sup>.

Reactants	Method/Basis	$\Delta G^\ddagger$ <sup>a,b</sup>		$\Delta\Delta G^\ddagger$ <sup>a,b,c</sup>
		C1-attack	C2-attack	
<b>11</b> + AlH <sub>4</sub> <sup>-</sup>	B3LYP/6-31+G*(PCM)	30.2	34.2	4.0
<b>11-Li<sup>+</sup></b> + AlH <sub>4</sub> <sup>-</sup>	B3LYP/6-31+G*(PCM)	6.8	10.0	3.2
	MP2/6-31+G*(PCM)//B3LYP/6-31+G*(PCM)	8.3	12.3	4.0
	wb97xd/6-31+G*(PCM)//B3LYP/6-31+G*(PCM)	7.4	11.1	3.6
	B3LYP/6-311+G(2d,p)(PCM)//B3LYP/6-31+G*(PCM)	7.2	10.2	3.0
	mPW1PW91/6-311+G(2d,p)(PCM)//B3LYP/6-31+G*(PCM)	8.5	11.7	3.2

<sup>a</sup>All energies are in kcal/mol and relative to separated reactants (**11** or **11-Li<sup>+</sup>** and AlH<sub>4</sub><sup>-</sup>). <sup>b</sup>Free energy corrections to electronic energies calculated at 298 K. <sup>c</sup> $\Delta\Delta G^\ddagger = \Delta G^\ddagger_{C2} - \Delta G^\ddagger_{C1}$

**Figure 1:** Reaction coordinate of ring opening of **11-Li<sup>+</sup>** with AlH<sub>4</sub><sup>-</sup>



Structures are optimized at B3LYP/6-31+G\*(PCM). Relative free energies (298 K) are given in kcal/mol.

For the lithium complex of cyclohexene oxide (**11-Li<sup>+</sup>**), the coordinated lithium could adopt two orientations, *endo*- (towards the (CH<sub>2</sub>)<sub>4</sub> portion of cyclohexene oxide ring) or *exo*- (away from the (CH<sub>2</sub>)<sub>4</sub> portion). Our calculations indicated that the *exo*-conformer (**11-Li<sup>+</sup><sub>exo</sub>**) was lower in energy than the *endo* conformer by 0.9 kcal/mol. We then explored the ring opening pathways for **11-Li<sup>+</sup>** with AlH<sub>4</sub><sup>-</sup> as the nucleophile. Our attempts to locate chair-like and twist-boat-like ring-opening transition structures with lithium in the *endo* orientation proved unsuccessful, as all these structures converged to the corresponding *exo*-structures (Figure 1).

Activation free energies ( $\Delta G^\ddagger$ ) for reaction of **11-Li<sup>+</sup><sub>exo</sub>** with AlH<sub>4</sub><sup>-</sup> were 6.8 kcal/mol for **11-TS<sub>1</sub>** (chair-like transition state), and 10.0 kcal/mol for **11-TS<sub>2</sub>** (twist-boat-like transition state), nearly 25 kcal/mol lower in energy than those for reaction of neutral **11**, indicating the mechanistic importance of Li<sup>+</sup> activation. The preference for the chair-like transition structure ( $\Delta\Delta G^\ddagger$ ) was 3.2 kcal/mol, similar to the preference seen by Nakamura and Morokuma for reaction of cyclohexene oxide with MeCuLi•LiCl (UB3LYP/6-31A).<sup>5</sup>

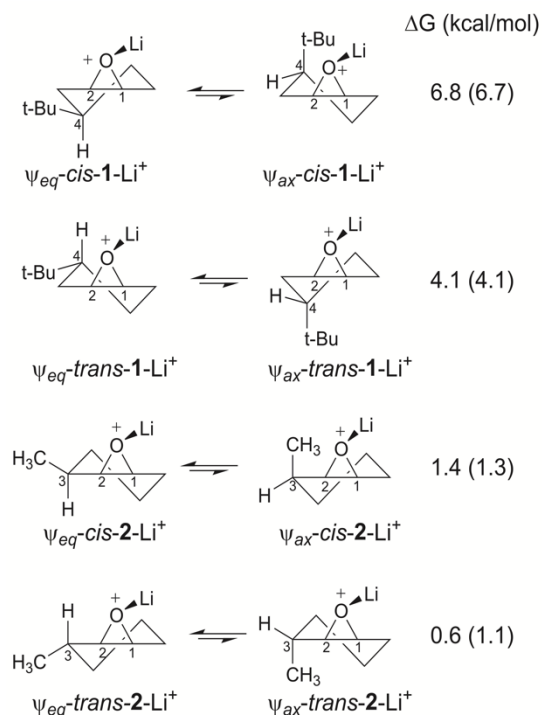
The preference for the chair-like transition structure in reaction of **11-Li<sup>+</sup><sub>exo</sub>** with AlH<sub>4</sub><sup>-</sup> did not change significantly when  $\Delta\Delta G^\ddagger$  values were calculated using single point energies at MP2/6-31+G\*(PCM), wb97xd/6-31+G\*(PCM), B3LYP/6-311+G(2d,p)(PCM) and mPW1PW91/6-311+G(2d,p)(PCM), ( $\Delta\Delta G^\ddagger = 3.0$  to 4.0 kcal/mol (Table 1)).

Since the magnitude of preference for the chair-like transition state was not affected by use of alternate functionals, larger basis sets, or explicit electron correlation, all subsequent calculations in this paper focus on the B3LYP/6-31+G\*(PCM) method, occasionally comparing free energies derived from other methods.

As a prelude to locating hydride-opening transition structures for *cis*-1, *trans*-1, *cis*-2, and *trans*-2, we examined the conformational preference of the corresponding *exo*-Li<sup>+</sup> complexes and the free epoxides at B3LYP/6-31+G\*(PCM). As expected, in each case the pseudoequatorial conformer was lower in energy. However, the magnitude of this preference varied considerably depending on the size, position and relative configuration of the alkyl group. As expected, *t*-butyl-substituted epoxides *cis*- and *trans*-1 showed large pseudoequatorial preferences (6.8 and 4.1 kcal/mol for the *exo*-Li<sup>+</sup> complexes (Scheme 3). For methyl-substituted epoxides *cis*- and *trans*-2, the pseudoequatorial preferences were much less pronounced (1.4 and 0.6 kcal/mol for the *exo*-Li<sup>+</sup> complexes respectively). Note that the conformational preferences for the neutral epoxides (Scheme 3, values in parenthesis) are similar in all cases.

We then began our investigation of the possible ring-opening pathways of the *t*-butyl-pseudoaxial ( $\psi_{ax}$ ) and *t*-butyl-

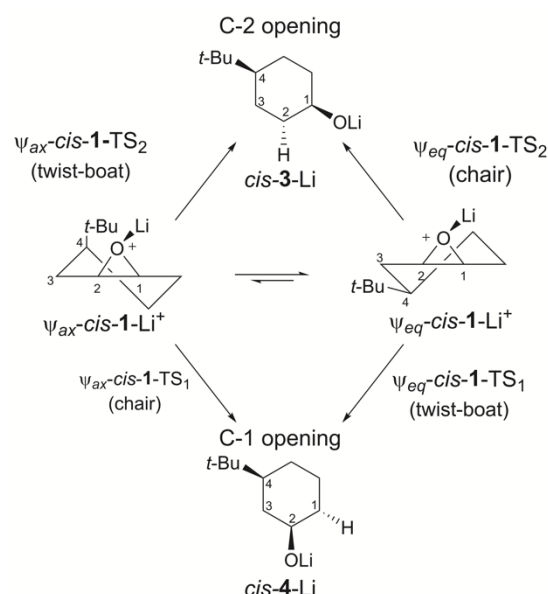
**Scheme 3:** Pseudoequatorial preference for lithiated (and neutral) *cis*- and *trans*-1 and 2



Geometry optimizations performed at B3LYP/6-31+G\*(PCM). Free energy corrections to electronic energies calculated at 298 K. Depicted free energies are in kcal/mol and are relative to the pseudoequatorial conformer; the pseudoequatorial preference of the corresponding neutral compounds is shown in parenthesis.

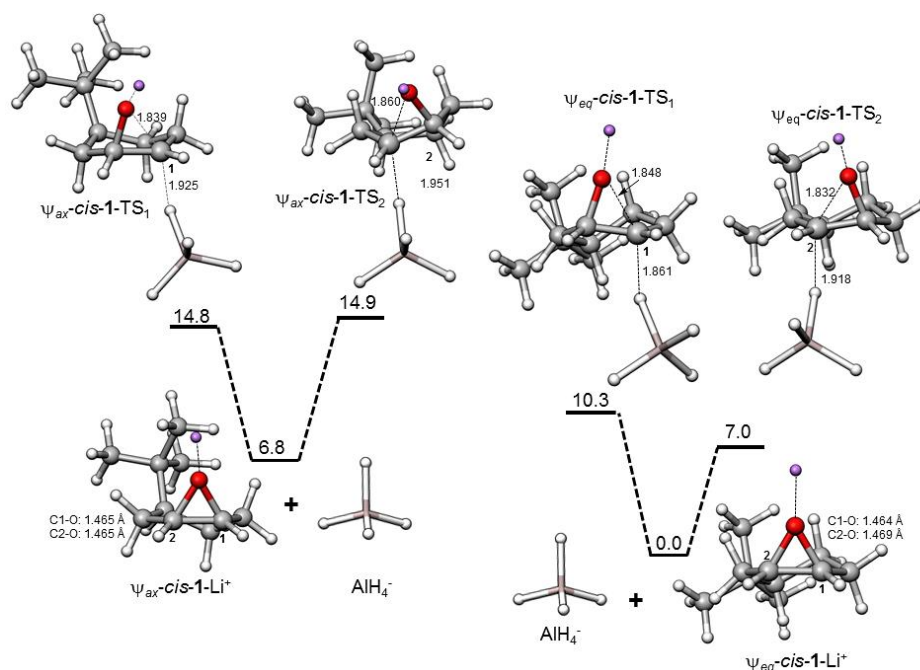
pseudoequatorial ( $\psi_{eq}$ ) conformers of *cis*-1 (Scheme 4). For  $\psi_{ax}\text{-}cis\text{-}1\text{-}Li^+$ , ring opening at C1 would proceed via a chair-like

**Scheme 4:** Possible ring opening pathways for *cis*-1-Li<sup>+</sup>



transition state to give product  $\psi_{ax}\text{-}cis\text{-}4\text{-}Li$ . In contrast, ring opening at C2 for  $\psi_{ax}\text{-}cis\text{-}1\text{-}Li^+$  will feature a twist-boat-like transition state yielding the product *cis*-3-Li. The opposite regiochemistry would be observed for  $\psi_{eq}\text{-}cis\text{-}1\text{-}Li^+$ , where C2-attack should be favored due to formation of the chair-like transition state, and C1-attack would occur via a twist-boat-like transition structure. Thus, ring opening at C2 should be favorable for  $\psi_{eq}\text{-}cis\text{-}1\text{-}Li^+$  with the *t*-butyl group in the pseudoequatorial position, and the opposite regiochemistry would be preferred for the pseudoaxial conformer  $\psi_{ax}\text{-}cis\text{-}1\text{-}Li^+$ .

We then located all four expected ring-opening transition structures for each epoxide at B3LYP/6-31+G\*(PCM). The four transition structures for *cis*-1 are shown in Figure 2:  $\psi_{eq}$  and  $\psi_{ax}$  designate the orientation of the *t*-butyl group, and TS<sub>1</sub> and TS<sub>2</sub> refer to hydride attack at C1 and C2 respectively. As expected, transition states featuring a pseudoaxial-*t*-butyl group ( $\psi_{ax}\text{-}cis\text{-}1\text{-}TS_1$  and  $\psi_{ax}\text{-}cis\text{-}1\text{-}TS_2$ ) were much higher in energy than  $\psi_{eq}\text{-}cis\text{-}1\text{-}TS_2$ . The same ordering and similar span of activation free energies was seen when single point energies of the four transition structures were calculated at MP2/6-31+G\*(PCM), wb97xd/6-31+G\*(PCM), B3LYP/6-311+G(2d,p)(PCM) and mPW1PW91/6-311+G(2d,p)(PCM) (Table S1, Electronic Supplementary Information). Similarly, the ordering and energetic span of transition structures was replicated using B3LYP/6-31+G\*(PCM) activation enthalpies (cf.  $\Delta\Delta H^\ddagger$  and  $\Delta\Delta G^\ddagger$  values in Table 1). Thus any errors in calculated  $\Delta S^\ddagger$  for these transition structures appear to be systemic and do not impact the predicted regioselectivity.<sup>27</sup> To conclude, at B3LYP/6-31+G\*(PCM), hydride attack at C2 is estimated to be >250-fold faster than attack at C1 (cf.  $k_f/k_s$  values), indicating almost exclusive formation of the C2 product (>99.9%) thus matching the experimental observation *cis*-1 reacts with LiAlH<sub>4</sub> at C2, giving *cis*-3 (Scheme 1).

Figure 2: Reaction coordinate for the ring opening of *cis*-1-Li<sup>+</sup> with AlH<sub>4</sub><sup>-</sup>

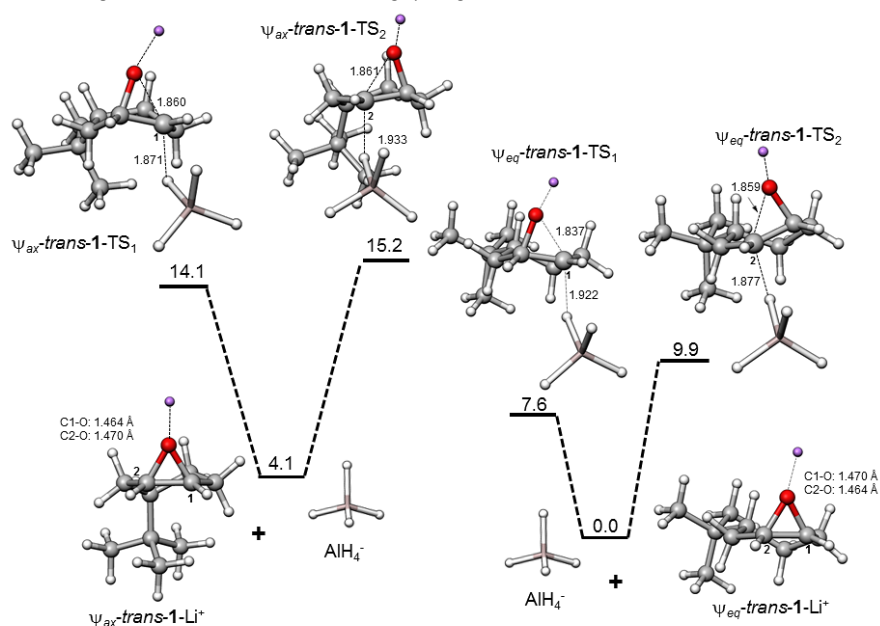
Structures optimized at B3LYP/6-31+G\*(PCM). Free energies provided in kcal/mol and relative to separated  $\Psi_{eq}\text{-}cis\text{-}1\text{-Li}^+$  and  $\text{AlH}_4^-$

**Table 2:** Free energies of activation at B3LYP/6-31+G\*(PCM) with ether for ring opening of compounds *cis*- and *trans*- 1 and 2 with  $\text{LiAlH}_4$  ( $\text{Li}^+\text{-O}$  bond in *exo* position).

	T.S.	$\Delta G^{\ddagger a,b}$	$\Delta\Delta G^{\ddagger c}(\Delta\Delta H^{\ddagger})$	$k_t/k_s$
<b><i>cis</i>-4-<i>t</i>-butyl</b>				
$\Psi_{ax}\text{-}cis\text{-}1\text{-TS}_1$	chair	14.8	7.8 (7.1)	0.0005
$\Psi_{ax}\text{-}cis\text{-}1\text{-TS}_2$	twist-boat	14.9	7.9 (7.3)	0.0004
$\Psi_{eq}\text{-}cis\text{-}1\text{-TS}_1$	twist-boat	10.3	3.3 (3.1)	1
$\Psi_{eq}\text{-}cis\text{-}1\text{-TS}_2$	chair	7.0	0.0 (0.0)	260
<b><i>trans</i>-4-<i>t</i>-butyl</b>				
$\Psi_{ax}\text{-}trans\text{-}1\text{-TS}_1$	twist-boat	14.1	6.5 (6.6)	0.0008
$\Psi_{ax}\text{-}trans\text{-}1\text{-TS}_2$	chair	15.2	7.6 (6.9)	<0.0001
$\Psi_{eq}\text{-}trans\text{-}1\text{-TS}_1$	chair	7.6	0.0 (0.0)	48
$\Psi_{eq}\text{-}trans\text{-}1\text{-TS}_2$	twist-boat	9.9	2.3 (2.7)	1
<b><i>cis</i>-3-methyl</b>				
$\Psi_{ax}\text{-}cis\text{-}2\text{-TS}_1$	twist-boat	11.3	3.6 (4.6)	0.14
$\Psi_{ax}\text{-}cis\text{-}2\text{-TS}_2$	chair	10.0	2.4 (2.1)	1
$\Psi_{eq}\text{-}cis\text{-}2\text{-TS}_1$	chair	7.7	0.0 (0.0)	59
$\Psi_{eq}\text{-}cis\text{-}2\text{-TS}_2$	twist-boat	10.4	2.7 (3.4)	0.65
<b><i>trans</i>-3-methyl</b>				
$\Psi_{ax}\text{-}trans\text{-}2\text{-TS}_1$	chair	8.6	0.4 (0.9)	1
$\Psi_{ax}\text{-}trans\text{-}2\text{-TS}_2$	twist-boat	13.3	5.1 (4.9)	<0.0001
$\Psi_{eq}\text{-}trans\text{-}2\text{-TS}_1$	twist-boat	10.6	2.4 (2.6)	0.03
$\Psi_{eq}\text{-}trans\text{-}2\text{-TS}_2$	chair	8.2	0.0 (0.0)	1.7

<sup>a</sup>All energies are in kcal/mol and relative to separated reactants ( $\Psi_{eq}\text{-}alkyl\text{-}cyclohexene\text{-}oxide\text{-}Li^+_{exo} + \text{AlH}_4^-$ ). <sup>b</sup>Free energy and enthalpy corrections to electronic energies calculated at 298 K. <sup>c</sup>Relative free energies ( $\Delta\Delta G^{\ddagger}$ ) and enthalpies ( $\Delta\Delta H^{\ddagger}$ ) of activation are very similar, indicating kinetic selectivities for ring opening are enthalpically driven.

The corresponding transition structures for *trans*-1 are shown in Figure 3; the lowest energy transition structure ( $\Psi_{eq}\text{-}trans\text{-}1\text{-TS}_1$ ) is chair-like and features attack at the C1 carbon of  $\Psi_{eq}\text{-}trans\text{-}1\text{-Li}^+$  conformer ( $\Delta G^{\ddagger}$  of 7.6 kcal/mol). The next lowest energy transition structure is for attack at the C2 carbon and is twist-boat-like  $\Psi_{eq}\text{-}trans\text{-}1\text{-TS}_2$  ( $\Delta G^{\ddagger}$  of 9.9 kcal/mol) with a relative activation barrier of 2.2 kcal/mol (Table 2). Once again, the transition structures featuring the pseudoaxial *t*-butyl group were considerably higher in energy, but interestingly in this case, the chair-like ( $\Psi_{ax}\text{-}trans\text{-}1\text{-TS}_2$ ) transition structure featured a higher activation energy ( $\Delta G^{\ddagger} = 15.2$  kcal/mol) than the twist-boat-like transition structure ( $\Psi_{ax}\text{-}trans\text{-}1\text{-TS}_1$ ,  $\Delta G^{\ddagger} = 14.1$  kcal/mol). This switch is likely due to the large 1,3-diaxial interaction of  $\text{AlH}_4^-$  with pseudoaxial *t*-butyl group in  $\Psi_{ax}\text{-}trans\text{-}1\text{-TS}_2$ , relative to the smaller 1,4-diaxial interaction seen in twist-boat-like  $\Psi_{ax}\text{-}trans\text{-}1\text{-TS}_1$ . This ordering of transition states was maintained using MP2/6-31+G\*(PCM), wb97xd/6-31+G\*(PCM), B3LYP/6-311+G(2d,p) (PCM) and mPW1PW91/6-311+G(2d,p)(PCM) single point energies (Table S1). Thus, based on our B3LYP/6-31+G\*(PCM) activation free energies, we estimate that hydride attack at C1 would occur >48 times faster than attack at C2, supporting the experimental observations that *trans*-1 reacts with  $\text{LiAlH}_4$  to give only *trans*-4 (and oxidation-reduction product *cis*-4) with no detected *trans*-3 (Scheme 1).

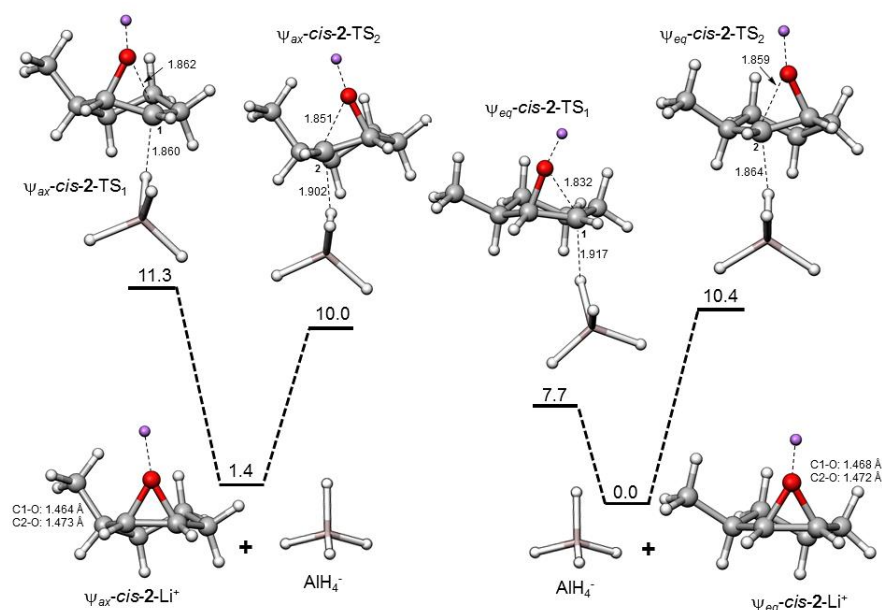
Figure 3: Reaction coordinate for the ring opening of *trans*-1-Li<sup>+</sup> with AlH<sub>4</sub><sup>-</sup>.

Structures optimized at B3LYP/6-31+G\*(PCM). Free energies provided in kcal/mol and relative to separated *trans*-1- $\psi_{eq}$ -Li<sup>+</sup> and AlH<sub>4</sub><sup>-</sup>.

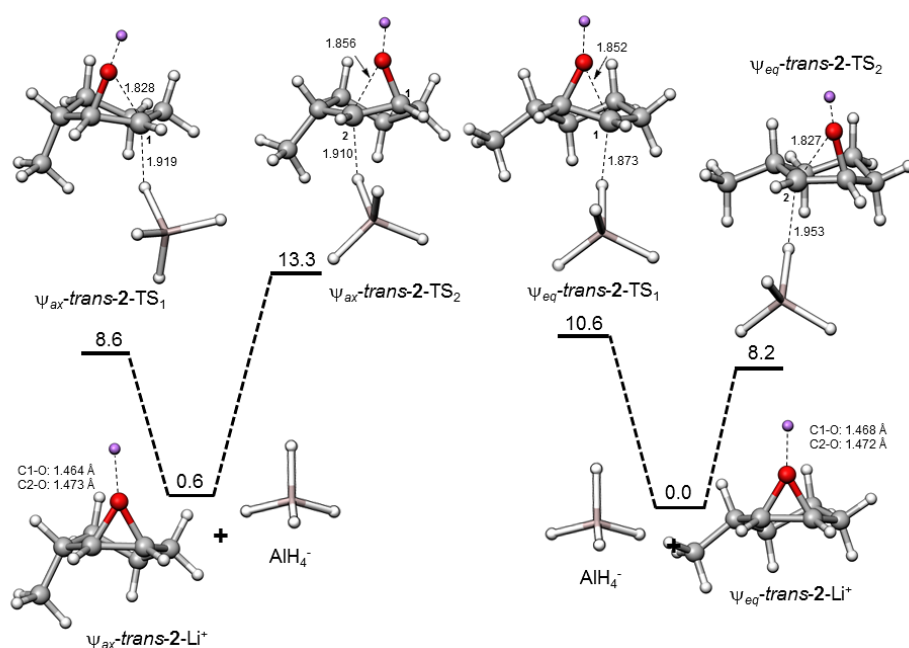
To test whether this selectivity would hold with a smaller alkyl group in the 4-position of cyclohexene oxide, we calculated the AlH<sub>4</sub><sup>-</sup> ring-opening transition structures for the lithium ion complexes of *cis*- and *trans*-4-methylcyclohexene oxides (*cis*- and *trans*-**12**). These calculations (See Table S5, Electronic Supplementary Information) predict >99:1 Fürst-Plattner control of AlH<sub>4</sub><sup>-</sup> ring-opening of both *cis*- and *trans*-**12**, mirroring the high selectivity observed for the *t*-butyl analogs *cis*- and *trans*-**1**. Thus at the 4-position of cyclohexene oxide, a large substituent is apparently not needed in order to achieve a high degree of Fürst-Plattner control. Unfortunately, to date

no experimental studies of AlH<sub>4</sub><sup>-</sup> ring-opening of stereochemically pure *cis*- or *trans*-**12** have been reported; thus these predictions cannot be confirmed.<sup>28</sup>

Next, we investigated the effects of methyl substitution at position 3 on the selectivity of ring-opening by AlH<sub>4</sub><sup>-</sup> (Figure 4). For *cis*-**2**, the chair-like transition structure ( $\psi_{eq}$ -*cis*-**2**-TS<sub>1</sub>) for attack at C1 is the lowest energy structure ( $\Delta G^\ddagger = 7.7$  kcal/mol). The next lowest energy structure is 2.4 kcal/mol higher in energy, and features attack at the C2 carbon via the chair-like transition structure  $\psi_{ax}$ -*cis*-**2**-TS<sub>2</sub> ( $\Delta G^\ddagger = 10.0$  kcal/mol) (Table 2). This data was again supported by all single point

Figure 4: Reaction coordinate for the ring opening of *cis*-2-Li<sup>+</sup> with AlH<sub>4</sub><sup>-</sup>.

Structures optimized at B3LYP/6-31+G\*(PCM). Free energies provided in kcal/mol and relative to separated  $\psi_{eq}$ -*cis*-**2**-Li<sup>+</sup> and AlH<sub>4</sub><sup>-</sup>.

Figure 5: Reaction coordinate for the ring opening of *trans-2*-Li<sup>+</sup> with AlH<sub>4</sub><sup>-</sup>.

Structures optimized at B3LYP/6-31+G\*(PCM), Free energies provided in kcal/mol and relative to separated  $\psi_{eq}$ -*trans-2*-Li<sup>+</sup> and AlH<sub>4</sub><sup>-</sup>.

calculations for all methods used (Table S1). For *cis-2*, hydride attack at C1 was estimated to occur >59-fold faster than attack at C2 (cf.  $k_f/k_s$ ). The calculated ratio for C1:C2 opening of 97:3 thus closely matches the observed 98:2 ratio of *cis-5* and *trans-6* to *cis-5* mentioned above (Scheme 1).

Gratifyingly, as observed experimentally, our calculations for *trans-2* predict reduced regioselectivity for reaction with LiAlH<sub>4</sub>. As shown in Figure 5, the lowest energy transition structure is for attack at C2 via the chair-like transition structure  $\psi_{eq}$ -*trans-2*-TS<sub>2</sub> with  $\Delta G^\ddagger$  of 8.2 kcal/mol (Table 2). Interestingly, the second lowest energy pathway, for attack at C1 through the chair-like transition structure ( $\psi_{ax}$ -*trans-2*-TS<sub>1</sub>), is only 0.4 kcal/mol higher in energy ( $\Delta G^\ddagger = 8.6$  kcal/mol). Thus, the rates of attack at C2 and C1 are comparable (i.e.  $k_f/k_s = 1.7$ ), and would thus provide a mixture of the major (*trans-5*) and the minor (*trans-6*) products in a 63:37 ratio, similar to the 70:30 ratio of *trans-* and *cis-5* to *trans-6* observed experimentally (Scheme 1). The small difference in energy between the two chair-like transition structures  $\psi_{eq}$ -*trans-2*-TS<sub>2</sub> and  $\psi_{ax}$ -*trans-2*-TS<sub>1</sub> seen at B3LYP/6-31+G\*(PCM) was again retained using single point calculations for all methods used, giving  $\Delta\Delta G^\ddagger$  values between 0.2 and 0.4 kcal/mol (Table S1).

The low regioselectivity for *trans-2* can be rationalized by the reduced pseudoequatorial preference observed for *trans-2*-Li<sup>+</sup> ( $\Delta G = 0.6$  kcal/mol, Figure 4). This reduced pseudoequatorial preference carries forward into poor (only 0.4 kcal/mol) energetic separation of the corresponding ring-opening chair-like transition structures  $\psi_{eq}$ -*trans-2*-TS<sub>2</sub> and  $\psi_{ax}$ -*trans-2*-TS<sub>1</sub>. The near-eclipsing interaction between the pseudoequatorial methyl group at C3 and the C2-H for  $\psi_{eq}$ -*trans-2*-Li<sup>+</sup> ( $H_3C-C_3-C_2-H$  dihedral =  $-19.7^\circ$ ) is only somewhat

relieved in  $\psi_{eq}$ -*trans-2*-TS<sub>2</sub> ( $H_3C-C_3-C_2-H$  dihedral =  $-31.5^\circ$ ). Thus torsional strain between C<sub>3</sub>-CH<sub>3</sub> and C<sub>2</sub>-H appears to play a role in destabilizing  $\psi_{eq}$ -*trans-2*-TS<sub>2</sub> just as Rickborn et al. had predicted for  $\psi_{eq}$ -*trans-2* itself.<sup>6</sup> The minor product (*trans-6*) would thus form through  $\psi_{ax}$ -*trans-2*-TS<sub>1</sub> ( $\Delta\Delta G^\ddagger = 0.4$  kcal/mol). Note that this near-eclipsing interaction is avoided in  $\psi_{eq}$ -*cis-2*, in which the pseudoequatorial C3-methyl and the C2-H are nearly staggered ( $H_3C-C_3-C_2-H$  dihedral =  $59.7^\circ$ ). Consequently there is strong Fürst-Plattner control for ring opening of *cis-2* and low Fürst-Plattner control of opening of *trans-2*.

## Conclusions

In conclusion, we located ring-opening transition structures for the reactions of 4-*t*-butylcyclohexene oxides (*cis-* and *trans-1*), 4-methylcyclohexene oxides (*cis-* and *trans-12*) and 3-methylcyclohexene oxides (*cis-* and *trans-2*) with LiAlH<sub>4</sub>. The computed transition structure free energies predict a high degree of Fürst-Plattner control for ring-opening of *cis-1*, *trans-1* and *cis-2* by LiAlH<sub>4</sub>, and low selectivity for *trans-2*, matching experimental observations. Although no experimental data exists to benchmark the calculations of *cis-* and *trans-12*, high regioselectivities are predicted in these two cases. The low regioselectivity seen experimentally for *trans-2* is attributed to the low pseudoequatorial preference observed in *trans-2* as a result of a near-eclipsing interaction between the pseudoequatorial C3-methyl and the C2-H (cf. Scheme 3, Figure 4). Thus, *trans-3*-alkyl cyclohexene oxides are expected to show reduced Fürst-Plattner selectivity, regardless of the size of the alkyl group. In contrast, *cis-3*-alkyl cyclohexene oxides, and both *cis-* and *trans-4*-alkyl cyclohexene oxides are

all generally expected to show high Fürst-Plattner selectivity in ring-opening reactions (cf. Table 2 and Table S5).

### Conflicts of interest

There are no conflicts to declare.

### Acknowledgements

This research was supported, in part, under National Science Foundation Grants CNS-0958379, CNS-0855217, ACI-1126113 and the City University of New York High Performance Computing Center at the College of Staten Island. Molecular graphics performed with UCSF Chimera, developed by the Resource for Biocomputing, Visualization, and Informatics at the University of California, San Francisco, with support from NIH P41-GM103311.

### Notes and references

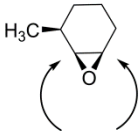
- G. H. Alt and D. H. R. Barton, *J. Chem. Soc.*, 1954, 4284.
- A. S. Hallsworth and H. B. Henbest, *J. Chem. Soc.*, 1957, 4604.
- C. W. Shoppee, D. N. Jones and G. H. R. Summers, *J. Chem. Soc.*, 1957, 3100.
- A. Fürst and A. Plattner Pl, *Helv. Chim. Acta*, 1949, **32**, 275-283.
- S. Mori, E. Nakamura and K. Morokuma, *J. Am. Chem. Soc.*, 2000, **122**, 7294-7307.
- B. Rickborn and W. E. Lamke, *J. Org. Chem.*, 1967, **32**, 537-539.
- B. Rickborn and S.-Y. Lwo, *J. Org. Chem.*, 1965, **30**, 2212-2216.
- G. Bellucci, G. Berti, M. Ferretti, G. Ingrosso and E. Mastrorilli, *J. Org. Chem.*, 1978, **43**, 422-428.
- G. Bellucci, G. Berti, G. Ingrosso, A. Vatteroni, G. Conti and R. Ambrosetti, *J. Chem. Soc. Perkin Trans. 2*, 1978, 627-632.
- B. Rickborn and J. Quartucci, *J. Org. Chem.*, 1964, **29**, 3185-3188.
- G. E. Garrett, K. Tanveer and M. S. Taylor, *J. Org. Chem.*, 2017, **82**, 1085-1095.
- P. Serrano, A. Llebaria, J. Vázquez, J. de Pablo, M. Anglada Josep and A. Delgado, *Chem. Eur. J.*, 2005, **11**, 4465-4472.
- C. J. Monceaux and P. R. Carlier, *Org. Lett.*, 2010, **12**, 620-623.
- M. Chini, P. Crotti, L. A. Flippin and F. Macchia, *J. Org. Chem.*, 1991, **56**, 7043-7048.
- M. Chini, P. Crotti, C. Gardelli and F. Macchia, *J. Org. Chem.*, 1994, **59**, 4131-4137.
- K. Tanveer, K. Jarrah and M. S. Taylor, *Org. Lett.*, 2015, **17**, 3482-3485.
- K. H. Hopmann, B. M. Hallberg and F. Himo, *J. Am. Chem. Soc.*, 2005, **127**, 14339-14347.
- H. Wang, K. N. Houk, D. A. Allen and M. E. Jung, *Org. Lett.*, 2011, **13**, 3238-3241.
- Gaussian [03,09], Revision C.02, M. J. Frisch, G. W. Trucks, H. B. Schlegel, G. E. Scuseria, M. A. Robb, J. R. Cheeseman, J. A. Montgomery, Jr., T. Vreven, K. N. Kudin, J. C. Burant, J. M. Millam, S. S. Iyengar, J. Tomasi, V. Barone, B. Mennucci, M. Cossi, G. Scalmani, N. Rega, G. A. Petersson, H. Nakatsuji, M. Hada, M. Ehara, K. Toyota, R. Fukuda, J. Hasegawa, M. Ishida, T. Nakajima, Y. Honda, O. Kitao, H. Nakai, M. Klene, X. Li, J. E. Knox, H. P. Hratchian, J. B. Cross, V. Bakken, C. Adamo, J. Jaramillo, R. Gomperts, R. E. Stratmann, O. Yazyev, A. J. Austin, R. Cammi, C. Pomelli, J. W. Ochterski, P. Y. Ayala, K. Morokuma, G. A. Voth, P. Salvador, J. J. Dannenberg, V. G. Zakrzewski, S. Dapprich, A. D. Daniels, M. C. Strain, O. Farkas, D. K. Malick, A. D. Rabuck, K. Raghavachari, J. B. Foresman, J. V. Ortiz, Q. Cui, A. G. Baboul, S. Clifford, J. Cioslowski, B. B. Stefanov, G. Liu, A. Liashenko, P. Piskorz, I. Komaromi, R. L. Martin, D. J. Fox, T. Keith, M. A. Al-Laham, C. Y. Peng, A. Nanayakkara, M. Challacombe, P. M. W. Gill, B. Johnson, W. Chen, M. W. Wong, C. Gonzalez, and J. A. Pople, Gaussian, Inc., Wallingford CT, 2004.
- A. Becke, *J. Chem. Phys.*, 1993, **98**, 5648-5652.
- J. Tomasi, B. Mennucci and E. Cancas, *Theochem-J. Mol. Struct.*, 1999, **464**, 211-226.
- J. Tomasi and M. Persico, *Chem. Rev.*, 1994, **94**, 2027-2094.
- For the sake of computational economy, at the outset we modeled Li<sup>+</sup>-etheral solvent interactions using implicit solvation. The Li<sup>+</sup> complexes of the epoxides and the resulting AlH<sub>4</sub><sup>-</sup> addition transition structures would likely exist as *tris*- (and possibly *tetrakis*-) diethyl ether solvates, and the vast conformational space of these solvates would be challenging to sample. Since PCM solvation gave such good agreement between calculated and observed ring-opening selectivities we did not pursue that approach.
- Kinetic product ratios calculated using the ratio of  $k_f/k_s$  values for all the C1 or C2 products obtained to the sum of  $k_f/k_s$  values for all products obtained.
- P. R. Carlier, N. Deora and T. D. Crawford, *J. Org. Chem.*, 2006, **71**, 1592-1597.
- E. F. Pettersen, T. D. Goddard, C. C. Huang, G. S. Couch, D. M. Greenblatt, E. C. Meng and T. E. Ferrin, *J. Comput. Chem.*, 2004, **13**, 1603.
- Bootsma and Wheeler have noted that activation free energies are particularly susceptible to error when the standard integration grids are used in DFT calculations, potentially impacting calculated stereo- and regioselectivity of reactions: see (Bootsma AN, Wheeler S. Popular Integration Grids Can Result in Large Errors in DFT-Computed Free Energies. ChemRxiv 8864204 [Preprint]. July 29, 2019. Available from: <https://doi.org/10.26434/chemrxiv.8864204.v5>). We see no evidence for such an effect here.

- 28 The reported  $\text{LiAlH}_4$  ring opening data was for a 1:1 mixture of *cis*- and *trans*-4-methylcyclohexene oxides and from these limited data it is impossible to extrapolate the regioselectivity of the pure diastereomers. See: B. Rickborn and S.-Y. Lwo, *J. Org. Chem.*, 1965, **30**, 2212-2216.

# Organic & Biomolecular Chemistry

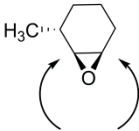
Page 10 of 10

*Why is Fürst-Plattner control of  $\text{AlH}_4^-$  reduction of *trans*-3-methylcyclohexene oxide so poor?*



98  
(97)

2  
(3)



30  
(37)

70  
(63)

Observed ratios  
Calculated ratios  
(B3LYP/6-31+G\*  
(PCM))